A HYBRID NEURAL NETWORK METHOD FOR MICROCALCIFICATION CLUSTER DETECTION IN MAMMOGRAPHY

A. Papadopoulos, D.I. Fotiadis, and A. Likas

11 – 2001

Preprint, no 11 – 01 / 2001

Department of Computer Science
University of Ioannina
45110 Ioannina, Greece

A hybrid neural network method for microcalcification cluster detection in mammography

A. Papadopoulos[1], D.I. Fotiadis[2] and A. Likas[2]

[1] Department of Medical Physics, Medical School
[2] Department of Computer Science
University of Ioannina, Greece

ABSTRACT: This paper introduces a microcalcification detection technique to be used as a part of a computer aided detection (CAD) scheme for mammographic images. The proposed method consists of several steps such as mammogram segmentation, microcalcification feature extraction and their cluster classification as true or false findings. It is tested on 20 mammograms of the MIAS mammographic database which contains microcalcification clusters. A hybrid neural network (HNN) system is used as a classifier consisting of a rule-based component followed by a feedforward neural network with one hidden layer that has been trained using the Levenberg-Marquardt algorithm. The achieved classification performance results in 94.1% sensitivity and 1.85 false positive clusters per image. The high microcalcification detection rate of the proposed system is a promising result indicating that the system could be exploited in the further development of a mammographic CAD system .

INTRODUCTION

Breast cancer is a major cause of women's death. Regular mammographic screening projects for women of certain age or high risk groups is taking place in developed countries. Mammography is the most reliable procedure for detecting nonpalpable cancers even when the size of the abnormality is minimal [1]. Early detection and removal of the primary tumor is an essential task that results in the reduction of patients modality [2]. However, it is difficult for a doctor to correctly diagnose a mammographic image. Therefore, several image processing techniques have been proposed to enhance mammographic images. Computerized methods have been developed to detect and classify possible lesions with the aim to become a "second opinion" for the radiologists in the process . mammographic diagnosis. One of the early signs of breast cancer is the presence of microcalcification clusters at the mammogram of asymptomatic women. However, a number of such findings could be missed or misinterpreted by doctors, due to the particularly small size and low contrast that they usually exhibit in an inhomogeneous mammographic background. At the same time, many diagnostic errors could occur, since the number of the expert radiologists is quite small and the interpretation of a mammogram could depend on radiologist's heavy schedule. Studies indicate that the radiologists' interpretation variability is about 8% as an average intraobserver, in addition to interobserver that is about 19% [3]. For all the above reasons, a reliable computer-aided diagnostic (CAD) tool could take place as a "second reader" at the procedure of mammogram interpretation.

In the literature, several techniques have been proposed to detect the presence of microcalcifications such as classical image processing methodologies [4,5,6], statistical methods [7], wavelet based techniques [8,9], and neural network techniques [10-16]. In our method, a segmentation technique is used to detect possible microcalcifications clusters (ROIs). For cluster identification a hybrid neural network system is used consisting of a rule-based component (with four rules) followed by a neural network component which is an one hidden layer feedforward classification neural network.

MATERIALS AND METHODS

Image data set

The mammographic database that is used for the development and evaluation of our technique is the database of the Mammographic Image Analysis Society (MIAS) [17]. Digitisation was performed on a Joyce-Loeble scanning microdencitometer SCANDIG-3, which has a linear response in the optical density range 0-3.2. Pixel depth is 8-bits with a spatial resolution of 0.05 pixel size. The images are categorized according to the biopsy-proven classes of their abnormality. Twenty-five of the images include microcalcifications that are localized with the help of a text data file containing for each cluster, the coordinates of the centre and the radius (in pixels) of a circle enclosing the abnormality. In three images, calcifications are widely distributed and in other two there was no biopsy indication. These five images were removed from our data set, which finally consists of ten malignant and ten benign microcalcification mammograms containing a set of twenty five localized microcalcification clusters (twelve malignant and thirteen benign) of several background tissues and sizes.

Skinline segmentation

In a typical mammogram one could identify different objects and areas such as the tissue area, the background space and a number of informative marks. The first step in each image processing methodology is the localization of the region of interest, that is the breast area. The removal of useless marks and image background regions is essential for the success of

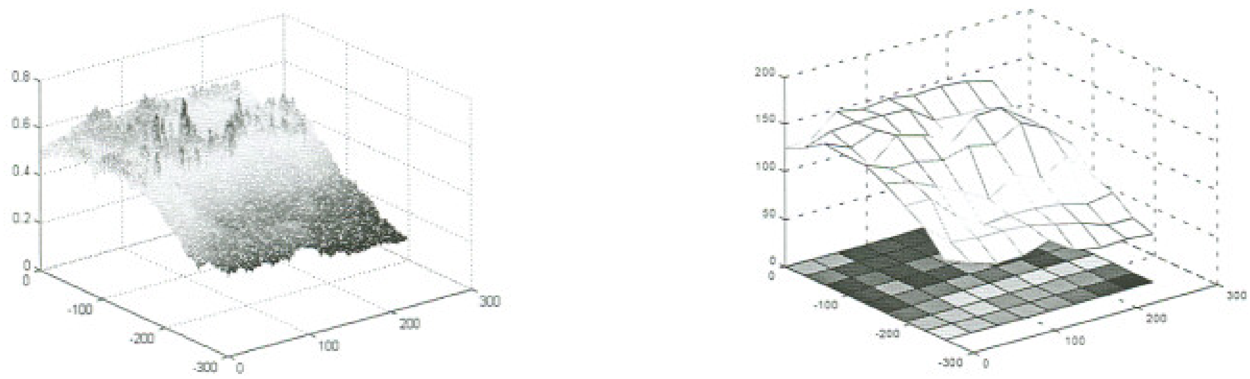

(a) (b)

Figure 1: (a) 3D representation of a grey value of 300×300 mammogram area, (b) Calculated background intensity of the same area.

further processing. The skinline segmentation procedure sets all the image pixels with intensity value less than 20 (for 8-bits scale, 0-255 grey levels) equal to zero. In this way, a binary thresholded image is obtained consisting of a number of "white" objects on a black background. The typical appearing objects are the breast region as well as several marks, identification letters or film artefacts on the background area. The area of each object is computed. The larger object corresponds to the breast region. All the pixels that belong to the breast area and are near to its boundary with the background area compose the skinline area. Close to the skinline a number of very small objects appears, that are actually parts of the breast region but due to the thresholding operation they appear as separate objects. Using morphological dilation, with a structure element radius of 30 pixels (~1.5 mm), an expansion of breast region outline is achived including the small objects that appear near to the breast outline along with all the pixels that are at the same area and have intensity values lower than 20. All the pixels that belong to the non-breast area take intensity values equal to zero and thus all the useless objects are removed from the image. In this way, the minimum rectangle that contains the breast region (bounding box) is automatically extracted and is used as the original mammogram for the subsequent steps.

Breast region segmentation

The segmentation process is possibly the most critical step on an image analysis method. Its aim is the segregation and the selection of the image parts that will be used for further processing. In our case, the regions of interest are the areas where microcalcifications exist. Thus, the outcome of the segmentation process is a number of localized pixels that are parts of possible microcalcifications in a specific region of interest (ROI).

A background correction method is applied to the mammogram after preprocessing. The image is considered as a 3D plot with the third axis corresponding to the intensity value of each pixel (Fig. 1a). The whole image is spitted into 30×30 subimages and through the use of bicubic interpolation in each subimage a second plot is computed. This plot represents the mean intensity level of each subregion that is an approach of the intensity level of the microcalcification local background (Fig. 1b). Then, the interpolated image is subtracted from the original mammogram producing a third image with each pixel value demonstrating the difference between the original and local background pixel values. Next, the pixels with the highest positive intensity differences are identified and a percentage of them is selected. The outcome image is in binary format. The reason for the selection of pixels with positive values is that the objects of interest (microcalcifications) are characterized by higher intensities compared to their background. The number of selected pixels is quite large since in subsequent processing a fraction of them will be removed. If the amount of the selected pixels is very low (lower than 10% of the total pixel number of the original image), the primary percentage become higher. Its value is chosen equal to the half of the pixel intensity that corresponds to the first percentage selection. In such a way a remarkable number of pixels will be included in the binary outcome image (A). The above case occurs when the mammogram has very low contrast usually due to erroneous exposure conditions.

The second step in the segmentation procedure is achieved using a contrast enhancement filter of a 9×9 kernel with its centre value equal to 80 and all the other values equal to –1 [18][19]. A selection of 5% of the more intensive pixels takes place, producing as a result an other binary image (B). The final segmented image is obtained from the logical summation (AND) of the two binary images, A and B. It contains the pixels that have high absolute intensity values and, at the same time, quite high intensity values in comparison with the background intensity of their local neighbourhood (Fig. 2).

Microcalcification detection and clustering

The pixels belonging to possible microcalcifications are identified in the segmented image as having unity value in contrast to the background pixels that are equal to zero. Neighbouring pixels with a connectivity of eight, are grouped together to create possible microcalcification objects. Objects that consist of less than two pixels are rejected since they are considered as noise [20]. Apart from the two-pixel objects, there is also a number of other small objects that are located over the breast area, are isolated and are quite far away from a larger microcalcification-size object.

Since the diagnostic information is related with the presence of object clusters, individual objects (possibly artefacts) should be removed. To eliminate these artefacts we apply morphological operators. Application of erosion using as structure element a 3×3 kernel with unity value, results in the removal of all objects apart from those that have at least one innermost pixel at the object's area that is not part of its boundary. After the erosion, only some inner pixels that belong to large area objects still

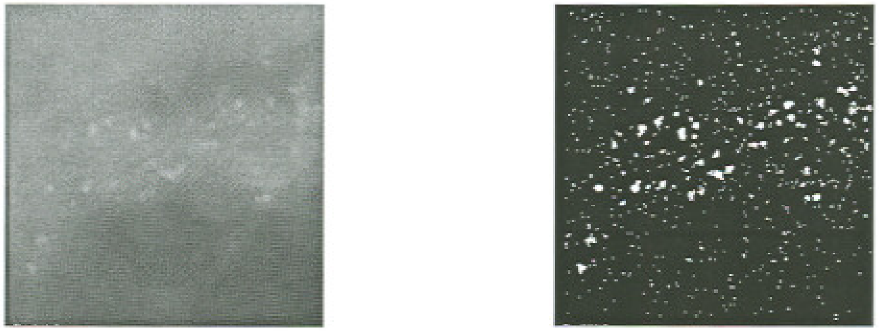

(a) (b)

Figure 2: (a) Representation of a part of mammogram. (b) The output of the segmentation algorithm of the image a.

remain. These pixels correspond to the centres of the regions of interest (ROIs), which will be generated using the dilation operator with a 3×3 structure element of unity value. The dilation is repeated for 50 times in order to produce a satisfying ROI area around the object. The smallest ROIs size is about 101×101 pixels and appears when the central object's pixel is olated and no other central pixel is located at a distance smaller than 100 pixels (100 pixels is the maximum allowed distance in order for two separate objects to belong in the same ROI). The distance value (100 pixels ~ 5 mm) is selected by taking into account the mean distance among microcalcifications in a cluster [21]. A ROI that is not of minimum size has been generated from a group of objects (possible cluster) that are located in the same neighbourhood. In such case, two or more ROIs will be connected and a new enlarged ROI will be generated containing more than two of the original objects. Based on the above methodology, several ROIs are identified in the mammoram and each of them is a candidate for being a real cluster of calcifications. The ROIs population is categorized in two classes depending on their area. The first group contains those ROIs with area lower than 20,000 pixels (2×100×100) (which is a reliable threshold value discriminating ROIs that are generated from individual objects). The second group contains the remaining ROIs having a remarkable area due to the inclusion of at least two nearby objects.

The problem that sometimes must be overcome is the existence of a small ROI near to a big one. In other words, the existence of an individual object close to a group of objects could be the case of an isolated microcalcification near to a large microcalcification cluster. To take into account this case, a second dilation process is applied on the previous dilated-ROIs image. It is applied only to the class of larger ROIs using a 3×3 structure element in a 50-cycles repeating step. The resulting image contains usually one or two ROIs that include at least one large ROI and perhaps some small ROIs that are close to the large area. The last step could provide information about small ROIs that exist close to large ROIs and are possibly part of them.

The physical meaning of the above procedure is an endeavour to localize a group of objects or possible microcalcification clusters. Cluster detection is the primary aim of radiologists in a mammogram interpretation procedure. The medical rule for the existence of microcalcification cluster in a location is the presence of more than three calcifications in 1 cm^2 area [22]. Using the above morphological analysis, a number of ROIs with different areas is extracted. The ROIs with small areas have low probability to correspond to real clusters but as the area becomes larger this possibility increases.

Feature calculation

A wide variety of features is automatically calculated for the objects (possible microcalcifications) and their corresponding groups - clusters. The computed features can be divided into three categories related with the object's intensity-contrast, shape and texture. Group features are calculated by considering each group as a large object with its shape formed from the outline of the area which encloses the individual objects. The group features are computed as the mean value of the five larger objects included in its area. The selection of the larger microcalcifications is done since a very small area microcalcification does not incorporate enough pixels for reliable feature value computation [21].

Table 1: Main features for cluster categorization.

Features for microcalcification (MC) cluster classification	**Radiologists characterization features**
Number of MCs in cluster	Cluster elements (separable / countable)
Cluster area	Cluster's size
Mean MC's area	MCs size
STD of MCs area	Shape of elements within cluster
Mean MC's compactness	Shape of elements within cluster
Mean MCs elongation	Shape of elements within cluster
STD of MC's elongation	Shape of elements within cluster
STD of MC's intensity	Density of calcifications
Mean MC's background intensity	Density of calcifications
Mean contrast	Contrast of calcifications
Cluster eccentricity	Shape of cluster
Mean distance from cluster centroid	Calcification's distribution
Neighbouring with a larger cluster	Calcification's distribution
Cluster Entropy	Calcification's distribution

Feature selection

The purpose of this step is the selection of features with the higher discriminative power. Through visual inspection we determined the features having the ability to categorize a high percentage of the cluster set. Additionally, the receiver operating characteristic (ROC) curve is plotted for each feature and the area A_z, under the ROC curve, is calculated. Features with the higher A_z area are collected. A set of 14 features that exhibit the highest discriminative performance is chosen (Table 1). The selected features are highly correlated with the mammographic features that radiologists examine during a diagnostic procedure [23].

Classification procedure

The aim of the classification component as part of the cluster detection procedure is the categorization of clusters identified during segmentation as true or false microcalcifications. The large number of false positive clusters that appears after the segmentation process, makes the classification task difficult. We propose a hybrid classification system consisting of a rule-based component followed by a neural network classifier.

Rule-based system

The rule-based approach was the first methodology employed in order to reduce the number of false positive microcalcification clusters [24][25]. In our rule-based component, combinations of main cluster features (listed in Table 1) are employed.

Neural network

Since classification efficiency of the rule-based system was not satisfactory, a methodology based on neural networks was tested. A multilayer feedforward neural network (multilayer perceptron) architecture is used. The network has an input layer with five nodes, one hidden layer -consists of 15 sigmoid nodes and an output layer with one sigmoid node. The input vectors are computed by considering the five principal components of the total set of computed features that contribute to the highest amount to the variation in the cluster feature set. Three main categories of training algorithms are tested. At the beginning, standard steepest descent and gradient descent with momentum are applied. Next, techniques with variable learning rate as well as resilient backpropagation algorithms are practiced. Finally, three types of numerical optimization techniques are implemented: the conjugate gradient, the BFGS Quasi-Newton method, and the Levenberg-Marquardt algorithm [26]. The training, as well as the test sets are equal to half of the whole cluster data set with each one containing approximately equal number of pathological clusters.

Hybrid neural network

The proposed hybrid artificial neural network methodology for the reduction of false positive detected clusters leads to improved performance efficiency compared to the single rule-based and neural network based schemes. The hybrid ANN consists of two main components (Fig. 3). The first one uses a set of four rules utilising the features with the highest discriminative power (with the largest A_z area under the ROC curve) to classify a significant number of "obvious" clusters. Obvious or typical [19] clusters are those which are easily evaluated by a radiologist as pathological. Clusters with many microcalcifications in a small area, having a high contrast with respect to their neighbourhood and particular shapes are clear cases of abnormalities.

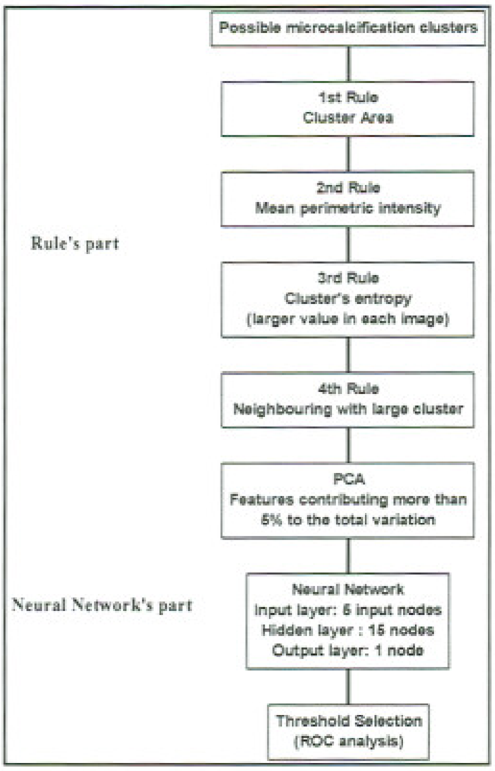

Figure 3: Representation of hybrid neural network.

The rule-based component of the HNN classifier uses four cluster features to identify typical clusters. The cluster area, mean boundary intensity, cluster entropy and neighbouring with large clusters are the features that are utilized. In what concerns the first two features, a threshold value is sufficient to distinguish large groups of real clusters. From the remaining clusters, we select the groups of objects with the highest entropy value in each mammogram and those that are located in the neighbourhood of a large cluster.

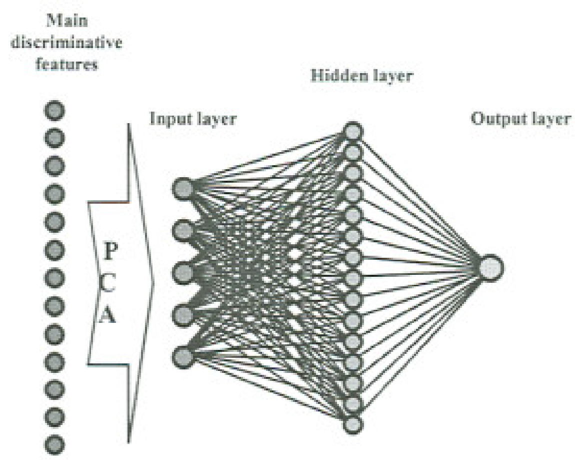

Figure 4: The neural network part of hybrid system.

The artificial neural network that is used as the second component of the HNN, is a three-layer feedforward neural network having an input layer with five nodes, one hidden layer with 15 nodes and an output layer of one node (Fig. 4). If the input vector includes all the main features of the Table 1 as its components, a high dimensionality vector is produced with highly correlated components. The components of feature vector are normalized to zero mean and unity variance. In order to reduce the dimensionality of the input vector principal component analysis (PCA) was applied to eliminate the components that contribute less that 5% to the total variation of the data set. The output of the PCA procedure is a five-component vector that constitutes the input to the neural network. The Levenberg-Marquardt algorithm in combination with Bayesian regularization is used for training [27][28].

RESULTS AND DISCUSSION

A set of 20 abnormal mammographic films of the MIAS database containing microcalcification clusters is used. Based on biopsy-proven characterization, 25 clusters has been classified as abnormal containing 12 malignant and 13 benign clusters. The output of our segmentation process, including all the MIAS true clusters, is 216 ROIs which are candidate microcalcification clusters. During the detection process, it is useful to maintain the sensitivity level as high as possible due to the specific diagnostic aim of the whole CAD application. Comparing the ground true cluster circles of the MIAS database with our segmented clustered images – binary images having value "1" in the ROIs area – we classified the ROIs as true or false findings. 34 detected ROIs belong to the 25 biopsy-proven circles of the database. This differentiation between the two sets is due to the fact that in some MIAS's localized circles more than one detected ROIs-clusters are included. Using the radiologists limitation that only clusters of three or more objects (within a region of approximately 1 cm^2) are considered as clinically suspicious [29], the number of ROIs that are candidate clusters is reduced to 193. In the next step, individual microcalcifications features as well as cluster features are extracted, as described above.

Table 2: Performance of several training algorithms for 88% sensitivity.

Training algorithm	Sensitivity	Specificity	False positive cluster / image
Gradient descent	0.88	0.59	3.25
Gradient descent with momentum	0.88	0.55	3.6
Resilient backpropagation	0.88	0.45	4.3
Conjugate Grad.	0.88	0.74	1.95
Scaled Conjugate Gradient	0.88	0.58	3.35
One Step Secant	0.88	0.66	2.7
Levenberg-Marquardt	0.88	0.52	3.85

The main subject of the following classification process is the reduction of the number of false positive clusters (fpc)-ROIs. The low specificity could be improved with the use of a classifier. Three approaches are implemented based on rule-based, neural network and hybrid neural network schemes. In the case of the rule-based classifier the implementation of thresholds in the features with the higher discrimination ability provide a reasonable reduction of fpc. The use of, at least, four rules on several feature sets, provides a correct classification for no more than 65% of the cluster set. The best performance is achieved using five features: cluster area, number of MCs in each cluster, cluster entropy and mean microcalcification's boundary intensity. Further improvement in categorization using a rule-based process is unfeasible due to the fuzzy boundaries at microcalcification features space. The necessity of better classification lead us to pursuit for a more sophisticated classification method.

Several topologies of a neural network classifier are tested using multilayer perceptron schemes applying one or two hidden layers. Their characterization performance is shown in Table 2. Better results are achieved using the conjugate gradient training algorithm. For sensitivity of 0.88 (4FN/34) the specificity is 0.74 or 1.95 fpc/image. Unfortunately when considering sensitivity 0.94 (2FN/34), the number of false positive clusters increased rapidly reducing the specificity to 3.95 fpc/image, which makes the network ineffective in high sensitivity procedures. Although the area under ROC curve (A_z) is amore convenient performance measure for the comparison of our networks, the number of false positive clusters at a specific sensitivity level is a significant descriptor of the classification success. The quantity A_z is not always an appropriate measure of performance because of its global nature, as pointed out in Ref. [30].

TABLE 3. Performance of several hybrid training algorithms at 88% and 94% sensitivity.

Training algorithm	Sensitivity	Specificity	False positive cluster / image
Gradient descent with momentum	0.88 (0.94)	0.70 (0.68)	2.4 (2.55)
Resilient backpropagation	0.88 (0.94)	0.65 (0.58)	2.75 (3.3)
Conjugate Gradient	0.88 (0.94)	0.71 (0.60)	2.25 (3.15)
Scaled Conjugate gradient	0.88 (0.94)	0.80 (0.62)	1.6 (3.0)
One Step Secant	0.88 (0.94)	0.66 (0.60)	2.7 (3.2)
Levenberg-Marquardt	0.88 (0.94)	0.80 (0.77)	1.55 (1.85)

The necessity for an even more effective classifier leads us to the construction of a hybrid system. The rule-based component is the same as described above. The performance of this step contributes to the correct classification of the "typical" clusters with a low number of mischaracterizations mostly in the false positive class. Testing with several network topologies as well as training algorithms was done for the classification of the rest – "atypical" clusters. The performance of the hybrid system is shown in Table 3. Although some of them have satisfactory performance only the Levenberg-Marquardt algorithm keeps a high specificity level for a range of sensitivity values. Scaled conjugate gradient has quite low fpc rate for 88% sensitivity, but at a higher level its specificity is low.

The hybrid system that has the best performance in a wide enough sensitivity range is the one contains a network with one hidden layer – 15 nodes trained with a Levenberg-Marquaridt algorithm. At a higher sensitivity of 0.94 (2FN/34) the specificity is 0.77 (37FP) or 1.85 fpc/image. The performance remains at the highest levels for a quite large range of networks sensitivities (Table 4). An additional measure of the system performance is the area A_z that is equal to 0.91.

Table 4: Performance of the proposed Hybrid Neural network trained with the Levenberg-Marquaridt algorithm.

Threshold	Sensitivity (FN)	Specificity	fpc/image
0.1	0.79 (7)	0.88	0.95
0.001	0.88 (4)	0.81	1.55
0.001	0.94 (2)	0.77	1.85
0.000001	0.97 (1)	0.73	2.15

Several techniques have been proposed demonstrating high false positive cluster detection performances. The comparison of their results is a difficult task since individual research groups use different datasets. Methodologies tested on the MIAS database have been reported in the literature [31,32]. The performance is at the same or lower level (with respect to our method) with the best one having a sensitivity value of 95.6% with 1.8 fpc/image. The computational time of our technique is quite low. Most time is spent during the segmentation process, that is about 30 min depending on the size of the breast area. Feature extraction and classification process are not time consuming (3 min).

CONCLUSIONS

A method for microcalcification detection in digitised mammograms based on computational feature extraction procedure is used in 20 images of MIAS database. A hybrid neural network system is used to reduce the high number of false positive detected microcalcification clusters. The achieved classification sensitivity of our technique is 94.1% with a false positive rate of 1.85 clusters per image.

Further testing has to be performed concerning the use of other databases as well as of original mammograms obtained from clinical routine or screening population projects. Additional analysis must be performed to assess the discriminating ability of the microcalcification features and their clinical evidence, in order to achieve categorisation between benign and malignant clusters.

ACKNOWLEDGEMENTS

The present work is supported by the Greek General Secretariat of Research and Technology as part of the project "EPET II – PENED Analysis and Design of classification methods for Computerized-aided detection of Breast cancer from radiological data".

REFERENCES

1. Zuckerman, H.C., The role of mammography in the diagnosis of breast cancer. *Breast Cancer, Diagnosis and Treatment*, Ariel, I.M., Cleary, J.B, Eds. New York: McGraw-Hill, 152-172 (1987).
2. Smith, R.A., *The epidemiology of breast cancer*. Syllabus: A categorical course in breast imaging RSNA, ed Kopans, D.B., Mendelson, E.B., 7-20 (1995).
3. Elmore, J.G., Wells, C.K., Lee, C.H., Variability in radiologists' interpretation of mammograms. *New Eng. J Med.*, 331, 1493-1499 (1994).
4. Chan, H.P., Doi, K., Galhotra, S., Vyborny, C.J., MacMahon, H., Jokich, P.M., Image feature analysis and computer aided diagnosis in digital radiography: 1. Automated detection of microcalcifications in mammography. *Med. Phys.*, 14, 538-548 (1987).
5. Dengler J., Behrens, S., Desage, J.F., Segmentation of microcalcifications in mammograms. *IEEE Trans. Med. Imag.*, 12, 634-642 (1993).
6. Clarke, L.P., Kallergi, M., Qian, W., Li, H.D., Clark, R.A., Silbiger, M.L., Tree-structured non-linear filter and wavelet transform for microcalcification segmentation in digital mammography. *Cancer letters*, 77, 173-181 (1994).
7. Kassemeijer, N., Adaptive noise equalization and recognition of microcalcifications in mammography. *Inter. J. Pattern Recog. Artif. Intel.*, 7, 1357-1376 (1993).
8. Yoshida, H., Doi, K., Nishikawa, R.M., Giger, M.L., Schmidt, R.A., An improved computer-assisted diagnostic scheme using wavelet transform for detection of clustered microcalcifications in digital mammograms. *Acad Radiol.*, 3, 621-627 (1996).
9. Strickland, R.N., Hahn, H.I., Wavelet transforms for detecting microcalcifications in mammography. *Proc. Int. Conf. Image Processing,* Austin, TX, 402-406 (1994).
10. Wu, Y., Giger, M.L., Doi, K., Vyborny, C.J., Schmidt, R.A., Metz, C.E., Artificial neural networks in mammography: application to decision making in the diagnosis of breast cancer. *Radiol*, 187, 81-7, (1993).
11. Patrick, E.A., Moskowitz, M., Mansukhani, V.T., Gruenstein, E.I., Expert learning system network for diagnosis of breast calcifications. *Invest Radiol.*, 26, 534-539 (1991).
12. Zheng, B., Qain, W., Clarke, L.P., Digital mammography: Mixed feature neural network with spectral entropy decision for detection of micocalcifications. *IEEE Trans. Med. Imag.*, 15, **5**, 589-597 (1996).
13. Nigel, R.H., Nishikawa, R.M., Papaioannou, J., Doi, K., Analysis of methods for reducing false positives in the automated detection of clustered microcalcifications in mammograms. *Med. Phys.*, 25, **8**, 1502-1506 (1998).
14. Lefebvre, F., Benali, H., Gilles, R., Kahn, E., Di Paola, R., A fractal approach to the segmentation of microcalcifications in digital mammograms. *Med. Phys.*, 22, **4**, 381-390 (1995).
15. Wu, Y., Doi, K., Giger, M.L., Nishikawa, R.M., Computerized detection of clustered microcalcifications in digital mammograms: application of artificial neural networks. *Med. Phys.*, 19, **3**, 555-560 (1992)
16. Veldkamp, W., Karssemeijer, N., Automated classification of clustered microcalcifications in digital mammograms: applications of artificial neural networks. Digital mammography. *Exerpta Medica*, 23-30 (1996).

17. Suckling, J., Parker, J., Dance. D., Astley, S., Hutt, I., Boggis, C., Ricketts, I., Stamatakis, E., Carneaz, N., Kok, S., Taylor, P., Betal, D., Savage, J., The mammographic images analysis society digital mammogram database. *Digital mammography* ed Gale, A.G., Astley, S.M., Dance, D.R., Cairns, A.Y., Amsterdam: Elsevier, 375-378 (1994).

18. Pratt, W.K., *Digital Image Processing*. Second Edition, A Wiley-Interscience Publication, John Wiley & Sons, Inc, (1991).

19. Schmidt, F., Sorantin, E., Szepesvari, C., Graif, E., Becker, M., Mayer, H., Hartwagner, K., An automatic method for the identification and interpretation of clustered microcalcifications in mammograms. *Phys. Med. Biol.*, **44**, 1231-1243 (1999).

20. Chan, H.P, Lo, S.C.B, Sahiner, B., Lam, K.L, Helvie, M.A., Computer-aided detection of mammographic microcalcifications: Pattern recognition with an artificial neural network. *Med. Phys.*, 22, **10**, 1555-1567 (1995).

21. Betal, D., Roberts, N., Whitehouse, G.H., Segmentation and numeral analysis of microcalcifications on mammograms using mathematical morphology. *Br J Radiol.*, 70, **9**, 903-917 (1997).

22. Kopans, D.B., *Breast Imaging*, Lippincott, J.B., Philadelphia, (1989).

23. Whatmough, P., Gale, A.G., Wilson, A.R.M., Do radiologists agree on the importance of mammographoc features?. *3rd Inter. Workshop on Digital Mammography*, 111-116 (1996).

24. Davies, D.H., Dance, D.R., Automated computer detection of clustered calcifications in digital mammograms. *Phys. Med. and Biol.*, 35, **8**, 1111-1118 (1990).

25. Chan, H.P., Doi, K., Vyborny, C.J., Schmidt, R.A., Metz, C.E., Lam, K.L., Ogura, T., Wu, Y., MacMahon, H., Improvement in radiologists' detection of clustered microcalcifications on mammograms: The potentioal of computer-aided diagnosis. *Invest. Radiol.*, 25, **10**, 1102-1110 (1990).

26. Bishop, C.M., *Neural Networks for Pattern Recognition*, Clarendon Oxford, Oxford University Press, 253-292 (1996).

27. MacKay, D.J.C., *Bayesian interpolation*, Neural Computation, 4, **3**, 415-447 (1992).

28. Foresee, F.D., Hagan M.T., Gauss-Newton approximation to Bayesian regularization. *Proc. Inter. Joint Conf. on Neural Networks*, 1930-1935 (1997).

29. Sickles, E.A., Breast calcifications: Mammographic evaluation. *Radiol.*, 160, 2, 289-293 (1986).

30. Metz, C.E., ROC methodology in radiologic imaging. *Invest Radiol.*, 21, **9**, 720-733 (1986).

31. Norhayati, I., Hiroshi, F., Takeshi, H., Tokiko, E., Automated detection of clustered microcalcifications on mammograms: CAD system application to MIAS database. *Phys. Med. Biol.*, **42**, 2577-2589 (1997).

32. Diahi, J.G., Frouge, C., Giron, a., Fertil, B., Artificial neural networks for detection of breast cancer in mammography. *3rd Inter. Workshop on Digital Mammography*. 329-334 (1996).